Tikrit Journal of Engineering Sciences (2023) 30 (3): 113-123

DOI: http://doi.org/10.25130/tjes.30.3.12

IRAQI Academic Scientific Journals

College of Engineering

ISSN: 1813-162X (Print); 2312-7589 (Online)

Tikrit Journal of Engineering Sciences

available online at: http://www.tj-es.com

TJES Tikrit Journal of Engineering Sciences

Synthesis, Design and Evaluation of Innovative Combined Nano-Catalysts Supported on Activated Carbon Prepared from Apricot Shells

Shymaa A. Hameed [a], Raja Ben Amar [b], Khaleel I. Hamad [c], Aysar T. Jarullah [d]*

a Gabes University, National Engineering School of Gabes, Tunisia.
b University of Sfax, Faculty of Science of Sfax, 3038 Sfax, Tunisia.
c Salah El-Din Study Center, The Open Educational College, Ministry of Education, Iraq.
d Chemical Engineering Department, College of Engineering, Tikrit University, Tikrit, Iraq.

Keywords:

Nano Catalyst; Catalytic Oxidative Desulfurization; Apricot shell/Activated Carbon; Fuel Oil.

ARTICLE INFO

Article history:

Received	10 June	2023
Received in revised form	04 July	2023
Accepted	07 July	2023
Final Proofreading	10 Aug.	2023
Available online	08 Sep.	2023

Citation: Hameed SA, Ben Amar R, Hamad KI, Jarullah AT. **Synthesis, Design and Evaluation of Innovative Combined Nano-Catalysts Supported on Activated Carbon Prepared from Apricot Shells**. *Tikrit Journal of Engineering Sciences* 2023; **30**(3): 113-123.
http://doi.org/10.25130/tjes.30.3.12

Corresponding author:

Aysar T. Jarullah

Chemical Engineering Department, College of Engineering, Tikrit University, Tikrit, Iraq.

Abstract: Clean fuel oil is crucial for a healthy environment and modern life. Therefore, removing sulfur-containing compounds is an effective issue using various techniques for desulfurization. In this study, the oxidation desulfurization (ODS) process was utilized with respect to the prepared new activated carbon (AC) made from apricot shells (AS) loaded by two combined active metals (Nickel-Cobalt-Manganese (NCM) and Nickel-Cobalt-Manganese-Molybdenum (NCMM)). Several characteristics related to the catalysts prepared (mainly SBET, pore volume, FTIR, TGA, SEM, EDX and XRD) have been investigated to analyze the produced nanocatalysts. The new nanocatalysts (NCM/AC and NCMM/AC) were generated by using the impregnation wetness incipient (IWI) method and evaluated for their ability to remove sulfur compounds from whole-cut fuel (from 29-345 °C) based on the air as an oxidant within batch reactor under the following conditions: air flow rate = 2 lit/min, reaction temperature = 90 °C, and reaction time of 60 min for both catalysts. It was found that Nano catalyst NCMM/AC performed better overall in removing sulfur components (57.29 %) than Nano catalyst NCM/AC (44.75 %), and excellent properties have been observed.

تحضير وتصميم وتقييم محفزات نانوية مبتكرة والمدعومة بالكربون النشط المحضر من قشور المشمش

شيماء علي حميد [1]، رجاء بن عمر[2]، خليل عيدان حمد [3]، أيسر طالب جارالله [4]
[1] المدرسة الوطنية للمهندسين بقابس / جامعة قابس / قابس- تونس.
[2] كلية العلوم بصفاقس /جامعة صفاقس/ صفاقس - تونس.
[2] كلية التربية المفتوحة، صلاح الدين/ تكريت - العراق.
[2] قسم الهندسة الكيمياوية / كلية الهندسة / جامعة تكريت / تكريت - العراق.

الخلاصة

زيت الوقود النظيف أمر بالغ الأهمية لبيئة صحية وحياة حديثة. لذلك، تعد إزالة المركبات الحاوية على الكبريت امر ضروري باستخدام تقنيات مختلفة لإزالة الكبريت. في هذه الدراسة، تم استخدام عملية إزالة الكبريت بالأكسدة (ODS) فيما يتعلق بالكربون المنشط الجديد (AC) المصنوع من قشور المشمش (AS) المحملة بمعدنين نشطين (نيكل - كوبالت - منغنيز (NCM) ونيكل - كوبالت - المنغنيز - الموليبدينوم (NCMM)). تم فحص العديد من الخصائص المتعلقة بالمحفزات المحضرة (بشكل أساسي S_{BET}، وحجم المسامة، وFTIR، وTGA، وSEM، وEDX، وXRD) لتحليل المحفزات النانوية المنتجة. تم إنشاء المحفزات او العوامل النانوية الجديدة (NCM / AC وNCMM / AC) باستخدام طريقة ال IWI (Impregnation Wetness Incipient) وتقييم قدرتها على إزالة مركبات الكبريت من الوقود المقطر الواسع (درجة غليانه من 29 الى 345 درجة مئوية) على أساس الهواء كمادة مؤكسدة داخل مفاعل دفعي في الظروف التالية: معدل تدفق الهواء = 2 لتر / دقيقة، ودرجة حرارة التفاعل = 90 درجة مئوية، وزمن التفاعل 60 دقيقة لكلا المحفزات المحضرة عمليا. وجد أن محفز النانو NCMM / AC كان بشكل عام أفضل في إزالة المركبات الكبريتية (57.29٪) من محفز النانو NCM / AC (44.75٪)، وقد لوحظت خصائص ممتازة له بالمقارنة مع العامل المساعد الاخر.

الكلمات الدالة: عوامل مساعدة ثانوية، إزالة الكبريت بالأكسدة التحفيزية، قشور المشمش، الكربون المنشط.

1.INTRODUCTION

A complex mixture known as crude oil mainly comprises hydrocarbons; however, it also contains small but important amounts of molecules containing metals, sulfur, oxygen, and nitrogen. Crude oil remains the main energy source worldwide, making up around 50% of the overall energy supply [1, 2]. The sulfur concentration of crude oil typically ranges from 0.05 to 10 weight %, although most often, it ranges between 1 and 4 weight % [3]. Sweet or low-sulfur crude oils have less than 0.5 weight % of sulfur, while sour or high-sulfur crude oils include more than 1 weight %. The main categories of sulfur compounds found in crude oil include organic compounds, such as thiophenes (T), mercaptans, sulfides, disulfides, benzothiophene (BT), dibenzothiophene (DBT), and so forth; [4] besides inorganic compounds, such as dissolved pyrites, hydrogen sulfide, and carbonyl sulfide [5, 6]. Due to growing knowledge of the harmful effects of burning sulfur-containing oils on human health and the environment, sulfur removal from transportation fuel and petrochemicals is receiving more attention [7]. One of the main causes of air pollution is specifically the presence of sulfur-containing compounds in transportation fuels, such as sulfides, disulfides, and thiophenes, which typically produce SOx [8]. Using metal catalysts in automobiles causes actual damage from excess sulfur compounds, including a decrease in the lifetime and activity of the catalytic converters [9]. Also, the health of humans is affected by several sulfur compounds when exposed to heavier thiophenes at specific levels, and they can cause cancer. Thiols also have an offensive odor, can affect breathing, irritate the eyes, throat, and lungs, cause coma, and lead to muscle spasms and nausea [10]. Therefore, many methods have been used to remove sulfur-containing components from fuel oil (desulfurization), including oxidative desulfurization (ODS), extraction, adsorption, hydrodesulfurization (HDS), and biodesulfurization (BDS) [10-13]. To achieve extensive desulfurization, sulfur compounds like mercaptan, benzothiophene, dibenzothiophene (DBT), and their alkylated derivatives must be removed. Oxidative desulfurization (ODS) has grown significantly in popularity because it efficiently eliminates aromatic sulfur compounds from fuels in mild conditions [14]. The oxidative desulfurization (ODS) strategy employs ambient pressure and temperature to address HDS issues [15]. For ODS, an effective catalyst is crucial. Thus, to make more efficient catalysts for boosting catalytic activity, hazardous pollutants created by various industrial processes, including petroleum refineries, must be reduced. Creating an environmentally friendly fuel with respect to minimum pollutants, which has recently become a significant issue in our lives, is significantly impacted by the choice of the catalyst type, their manufacturing process, and the selection of materials in their composition [16]. By changing the textural characteristics of the catalyst, it is possible to efficiently modify the catalytic activity of supported metal oxides [16]. Compared to supports with weak morphological properties, the excellent morphological properties typically encourage the dispersion of metal oxides, boosting the activity of metal oxide in chemical processes. To

obtain a highly active and selective catalyst, all of these conditions must be present. Activated carbon (AC) is one of the most significant materials that can be used with confidence to design catalysts (or active supports) due to its highly porous material with inherently high surface area and high pore volume [17]. Activated carbons (ACs) are frequently used to reduce the concentration of environmentally hazardous pollutants. Apricot shells, a sustainable and affordable alternative, are only one of the many precursors that can be used to create ACs. The chemical makeup and study of the apricot shells revealed that they were an excellent source of material for producing activated carbon [18]. AC-based catalysts are potential methods to keep ODS processes adhering and active at their best metals. Nickel, cobalt, manganese, and molybdenum oxides are believed to work best when supported together by AC to provide a highly efficient catalyst. As a result, the catalyst system for the ODS process becomes much more cost-effective. The composite catalyst acts as an oxidant, combining with air or oxygen to create an intermediate product more effective at oxidizing sulfur compounds prevalent in fuel oils [19]. In the present work, apricot shell stones are employed to generate the AC as a support for generating the catalysts needed. Then, various metal oxides for preparing such new nanocatalysts, namely manganese (Mn), cobalt (Co), nickel (Ni), and molybdenum (Mo), were loaded on AC to obtain the required nanocatalysts (which are NCM/AC and NCMM/AC). After that, an effective catalytic oxidative desulfurization method was used via air as an oxidant and batch reactor as a reaction system to reduce the sulfur content in whole-cut fuel (middle distillates).

2.EXPERIMENTAL PROGRAM

2.1. Materials

Nickel acetate tetrahydrate (CH3COOH)2Ni.4H2O, Cobalt chloride hexahydrate (CoCl2.6H2O), Manganese (III) acetate hydrate ((CH3COO)2 Mn.2H2O), Ammonium Molybdate tetrahydrate ((NH4)6Mo7O24. 4H2O) were used as main resources for preparing the catalysts (purchased from Thomas Baker, UK with a purity of 99%). Deionized water was supplied by the analytical chemistry lab (at Chemical Engineering Department/Tikrit). The whole-cut fuel that contains sulfur (0.4826 wt%) was obtained from North Refineries Company (Baiji refinery) / Iraq. It is used as an oil feedstock and air as an oxidant for the ODS reaction test. The physical characteristics of the whole cut fuel are described in Table 1 and tested by North Refineries Company laboratories/ Iraq.

Table 1 The Physical Characteristics of the Whole Cut Fuel.

Variable	Unit	Value
Specific gravity @15.6 °C	-	0.7708
API	-	52.08
Initial boiling point	°C	29
End boiling point	°C	345
Sulfur content	wt%	0.4826
Density @ 20 °C	g/cm^3	0.7669
MeABP	°C	168.247
Molecular weight	g/gmole	139.276
Viscosity @ 40°C	cSt	1.091

2.2. Preparation of Nano Catalyst

2.2.1. Preparation of Activated Carbon

Local apricots were used to prepare the activated carbon. A pretreatment involved apricot stones that were first washed with hot water to remove dirt from their surface and then dried under sunlight for a few days. The dried stones were crushed to obtain the outer shell of these stones and ground using a laboratory mill. The powdered material was next screened to desire sizes under 425 µm (40 mesh). Afterward, the chemical treatment included two steps: First, treatment with phosphoric acid (H3PO4), the weight ratio of (AS: H3PO4) was (1:2), and the AS was impregnated with (H3PO4) solution at (70℃) for 24 hr using a magnetic heater stirrer. The mixture was dried at 110°C overnight in an oven to complete acid evaporation. The sample was washed with hot deionized water (DI), and the washing solution was measured by a pH until it became neutral. After that, the sample was subjected to carbonization and an activation process by a tubular furnace at 500°C for 2 hr and pure nitrogen (99.995%) was flowed to prevent carbon combustion. The second treatment was conducted with nitric acid (HNO3) at impregnation concentration (50%) with a weight ratio of AC:HNO3 (1:2) immersed for 2 hr at 70℃ using a magnetic heater stirrer. The mixture was washed with deionized water (DI), and the washing solution was secondly measured by a pH meter until it became neutral. Finally, the washed activated carbon was dried overnight at 110℃ in an oven.

2.2.2. Catalysts Preparation

The new combined nanocatalysts (NCM/AC) and (NCMM/AC) were created using the Impregnation Wetness Incipient (IWI) process. To prepare the first nanocatalyst (NCM/AC), a mixture containing (10%) of NCM (Nickel acetate tetrahydrate (16.96 g), Cobalt chloride hexahydrate (8.075 g) and Manganese (III) acetate hydrate (19.521 g)) was weighted in a beaker and dissolved in deionized water (1748.911 ml). Then, a magnetic stirrer was used to mix the solution for 30 min at room temperature to create a saturated solution. The homemade activated carbon nanoparticles were weighed in a beaker, added to the NCM solution, and stirred with a magnetic stirrer for 15 min at room temperature. An ultrasonic

homogenizer mixer (sonicator) was used, where the mixture was mixed entirely for 80 minutes and left overnight in the sonicator. After that, the mixture was heated at 60 °C with steady stirring until the water was fully evaporated; then, the impregnated activated carbon solution was loaded in a crucible and placed in an oven overnight to dry at 120 °C. After drying, the catalyst was calcinated in a tubular furnace at 850 °C for 2 h under N2 gas (99.99% purity). The second new combined nanocatalyst (NCMM/AC) was prepared by adding 2 wt% (2.4 g) of Ammonium Molybdate tetrahydrate (NH4)6Mo7O24. 4H2O) that was weighted in a beaker and dissolved in deionized water to the mixture at 8 wt% of NCM (Nickel acetate tetrahydrate (13.571 g), Cobalt chloride hexahydrate (6.460 g) and Manganese (III) acetate hydrate (15.617 g)). Then, the solution was mixed using a magnetic stirrer for 30 min at room temperature to create a saturated solution of (NCMM). The same procedure of the prepared nanocatalyst (NCM/AC) was repeated to obtain the nanocatalyst (NCMM/AC). Fig. 1 shows the NCM and NCMM preparation steps.

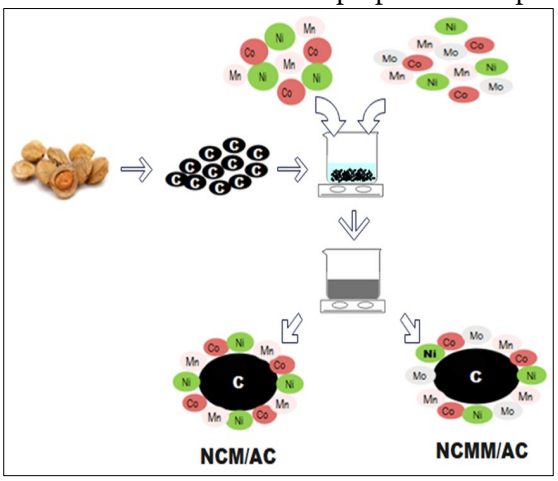

Fig. 1 Preparation Nano-Catalysts (NCM/AC) and (NCMM/AC).

2.2.3. *Characterization*

Several characterization methods were used to characterize the AC, NCM/AC, and NCMM/AC Nanocatalysts. The methods used to characterize the obtained catalysts are laid out in this part of the paper. Fourier Transform Infrared (FTIR) spectrophotometer, Energy Dispersive X-Ray (EDX), Thermogravimetric Analysis (TGA), X-ray diffraction (XRD), and Brunauer-Emmett Teller (BET) specific surface area, pore size distribution, and pore volume are some of the techniques used. The tests were conducted at the Petroleum Research and Development Center /Ministry of Oil/Iraqi laboratory.

2.3. *Catalysts Performance via ODS Reactions*

To test and evaluate the prepared catalyst for sulfur removal, a 500 ml jacketed round-bottom flask was used for the catalytic tests. It had a magnetic stirrer and a water bath with circulation to keep the temperature at 90℃, atmospheric pressure, airflow rate = 2 lit/min, and reaction time of 60 min. A vertical condenser was attached to the middle neck to condense the vapor. The second neck was utilized to allow the compressor-connected oxidant (air) to flow at a constant inlet pressure. The air was introduced into the flask through a glass tube to increase the contact between the gas, liquid, and nanocatalysts. The third neck was used to remove the sample when the reaction time was completed and to measure the temperature of the reaction in the flask by introducing a thermometer into the solution inside the flask. A 300 ml of whole-cut fuel (4826 ppm total sulfur) was used as the oil feedstock. In a typical run, the prepared catalyst (NCM/AC and NCMM/AC) and air were gradually dispersed in the feedstock (catalyst/whole cut fuel=0.01 g/ml) while being rapidly stirred. After 30 min, the mixtures were left at room temperature. The total sulfur was then calculated using an X-ray fluorescence sulfur analyzer after removing the samples. Fig. 2 shows the ODS batch reactor system. The sulfur content in the whole-cut samples was evaluated by ASTM D7039 in Petroleum Laboratory at Tikrit University-Iraq.

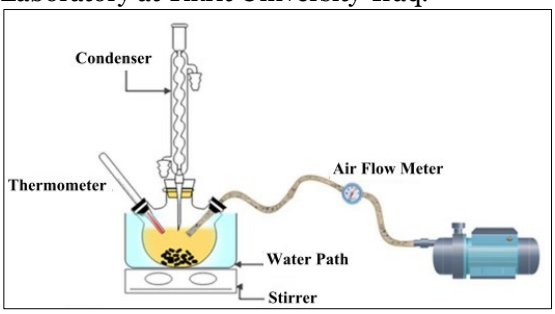

Fig. 2 Batch Reactor System.

3.RESULTS AND DISCUSSION

3.1. *Catalysts Efficiency*

Various attempts have been made to improve the activated carbon efficiency from apricot shells catalysts by using several transition metals, such as Co, Ni, Mn, and Mo, in the process of oxidation desulfurization. The effect of loading some of the transition metals on AC support was evaluated to identify the best nonporous catalyst for the ODS process. The first nanocatalyst (NCM) was made with total transition metals by 10 (wt%) mix of (2 (wt%) Co, 4 (wt%) Ni, and 4 (wt%) Mn) and 90(wt%) of AC as catalyst support. The second nanocatalyst (NCMM) was prepared with total transition metals of 10% (8 (wt%) mix of (Ni (3.2 wt%), Co (1.6 wt%), and Mn (3.2 wt%)) and 2% Mo (2 wt%)). With a feed sulfur content of 4826 ppm, the catalysts manufactured were evaluated in an ODS reaction. The best ODS catalyst was found to convert sulfur in the prepared nanocatalysts.

3.1.1. Pore Volume and BET Surface Area

Determining the catalysts' surface area and pore capacity is also essential since these characteristics might affect the catalytic activity and mass transfer of reactants and products [20]. The nitrogen adsorption-desorption method measured the S_{BET} and pore volume of activated carbon, nanocatalyst NCM/AC, and NCMM/AC adsorbents. These results are presented in Table 2.

Table 2 The BET Analysis for Support and Nano-Catalysts.

Catalyst Type	Surface Area m^2/g	Pore Volume cm^3/g	Average Pore diameter (nm)
AC	1133.347	0.648	37.92
NCM/AC	911.426	0.619	44.26
NCMM/AC	878.985	0.602	50.95

According to these results, the produced AC's surface area was 1133.347 m^2/g with a total pore volume and average pore diameter of 0.648 cm^3/g and 37.92 nm, respectively. Such new findings, which include the high surface area and pore volume of AC from homemade source (AS), are regarded as novel and inventive findings that have not yet been published in the literature and will favorably affect the catalysts produced. The specific surface area, total pore volume, and average pore diameter of AC were reduced to 911.426 m^2/g, 0.619 cm^3/g, and 37.92 nm, respectively, after impregnation with NCM. These reductions in the surface area, pore volume, and diameter of the mesopores are ascribed to NCM oxides occupying some of the AC's empty sites. Thus, decreasing in the possible S_{BET} for the adsorption process is available. With respect to the NCMM/AC catalyst, there was a limited reduction in the surface area and total pore volume of the catalyst to 878.985 m^2/g and 0.602 cm^3/g, respectively. This marginal decrease suggests that the impregnation of the NCMM material occurred predominantly on the catalyst's external surface. Hence, the coated material particles were not migrated to the interior pores. Furthermore, the decrease would insignificantly affect the surface area accessible for adsorption. In general, as the amount of the active component grows, the surface area of the catalytic material decreases until the monolayer coverage of the impregnated component is complete [21].

3.1.2. Analysis of Pore Size Distribution

The existence of mesopores and mesopores in the samples was indicated by the pore size distribution displayed in Fig. 3. The pore size distribution revealed two maxima at 22 and 56 nm (in all figures), showing the dominance of mesopores size at the first one and demonstrating the participation of macroporous at the second one with sizes ranging from 25-100 nm. Such AC high porosity from AS can slightly be attributed to the higher content of cellulose in the precursor (apricot seeds) since the source of the precursor has a significant impact on the pore structure of AC prepared by the one-step pyrolysis activation process that was employed in the present work [22].

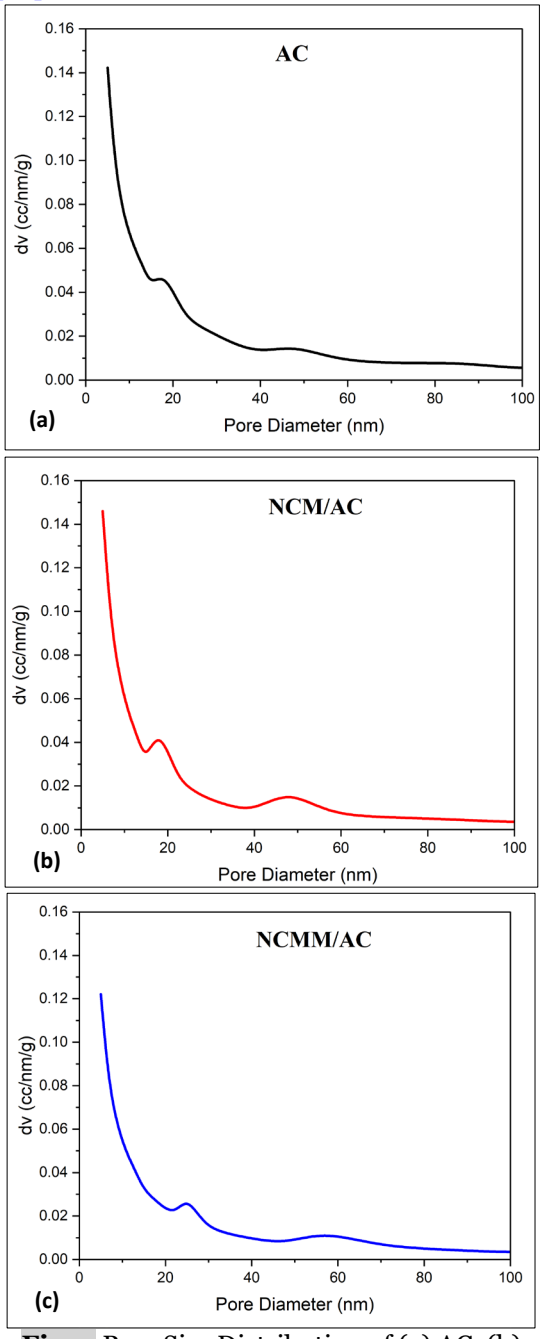

Fig. 3 Pore Size Distribution of (a) AC, (b) NCM/AC, and (c) NCMM/AC.

3.1.3. Analysis of SEM-EDX Data

All samples of nanocatalysts metals (Ni-Co-Mn) (NCM) over the surface of activated carbon support (AC) and metals (Ni-Co-Mn-Mo) over the surface of activated carbon support (AC) were tested by SEM-EDS. Fig. 4 shows SEM images of all nanocatalysts, where the metals are represented as white parts and nano-activated carbon support is represented as black parts. As clearly noted from these figures,

there were no metal agglomerations on the produced catalyst, and the metals were effectively distributed and impregnated. As a result, a more uniform impregnation was conducted. Moreover, the catalyst's particle size, shape, and porosity significantly influenced the reaction activity. The results suggest that the metal crystallite sizes for the NCM/AC sample were significantly lower than the NCMM/AC sample. Furthermore, such catalysts developed a porous texture due to H_2SO_4 evaporation during the carbonization step. A clear covering was also detected encircling these particles due to the added NCM and NCMM oxide material. The presence and dispersion of the active metal species on the catalyst substrate were verified by the EDX elemental mapping.

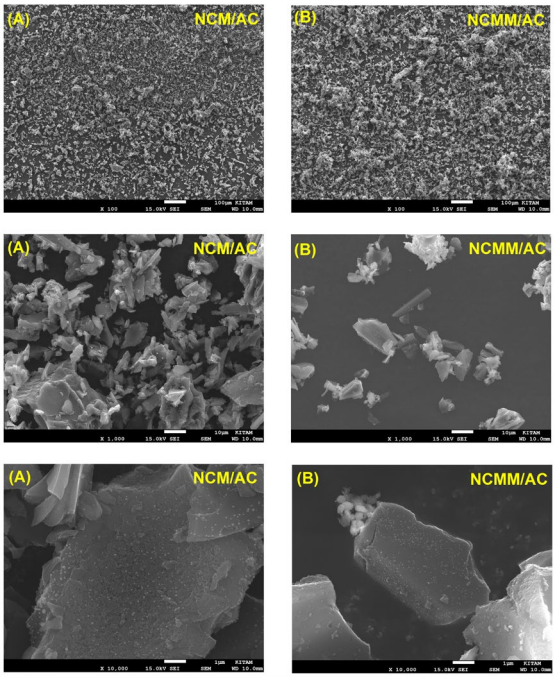

Fig. 4 SEM Images of (A) NCM/AC and (B) NCMM/AC.

Figs. 5-7 show the EDX elemental mapping, relative dispersion densities, and the elements presented on the surface of NCM/AC and NCMM/AC. These figures, regarding all nanocatalysts, have confirmed that the creation of metal nanocatalysts was observed by thermal and chemical degradation. According to the EDX analysis, all of the samples obtained by chemical and thermal ways indicated the development of different kinds of metal nanoparticles. Each sample contained metals like Ni, Mn, Co, and Mo, helping create metal nanocatalysts. The EDX examines demonstrated an attractive and uniform distribution of components on the catalysts' outer surface. The presence of C (73.1% wt%), O (14.2 wt%), Co (1.95 wt%), Mn (3.91 wt%), and Ni (3.89 wt%) was confirmed by the EDX mapping for NCM/AC, and C (71.7% wt%), O (17.4 wt%), Co (1.48 wt%), Mn (3.06 wt%), Ni (3.19 wt%), and Mo (1.91 wt%) for NCMM/AC. The limited change in surface area and pore volume values following the layering of the metal oxides material, as confirmed by the EDX, shows that such metal oxides were uniformly distributed on the surface of the NCM and NCMM over the AC catalyst without distorting the substance structure or affecting the pores created by AC activation. The weight % of the metal oxide material demonstrates that the techniques employed to apply the desired weight percent of such active components were implanted satisfactorily [23].

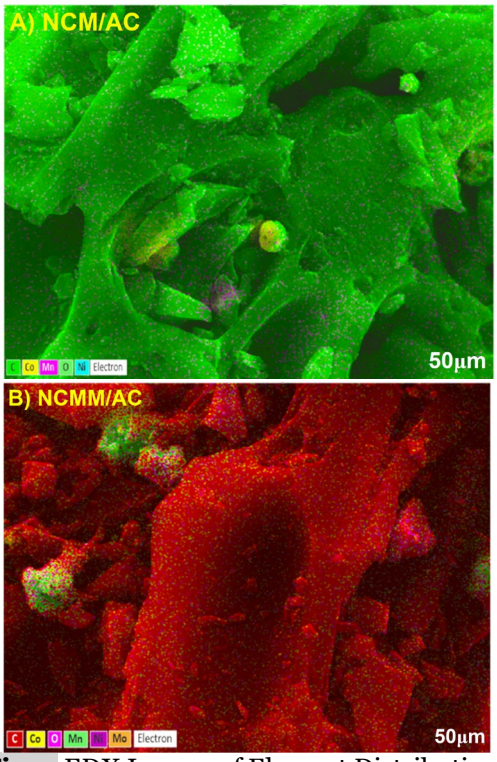

Fig. 5 EDX Images of Element Distribution of (A) NCM/AC and (B) NCMM/AC.

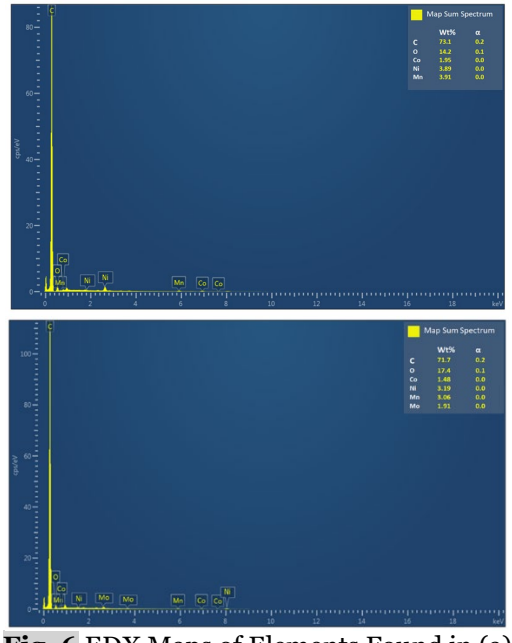

Fig. 6 EDX Maps of Elements Found in (a) NCM/AC and (b) NCMM/AC.

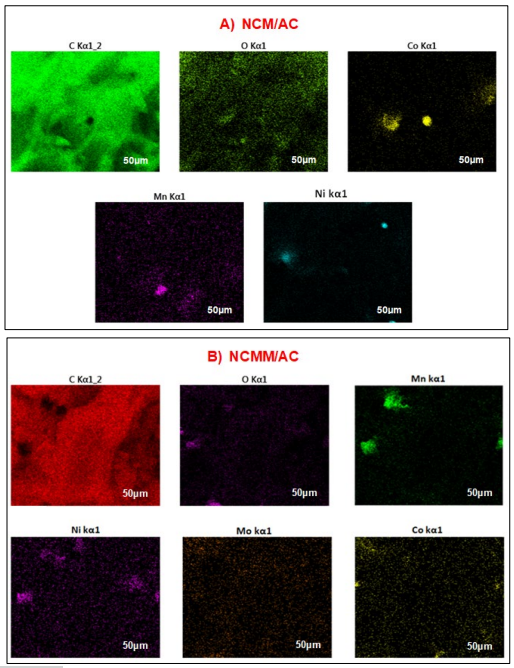

Fig. 7 Elements Existed on the Surface of (A) NCM/AC and (B) NCMM/AC.

3.1.4. Thermal Gravitational Analysis (TGA) Test

TGA, or thermographic analysis, parent materials and magnetic adsorbents' thermal gravimetric (TG) and derivative thermal gravimetric (DTG) curves of the nanocatalysts NCM/AC and NCMM/AC were studied by thermogravimetric analysis, as shown in Fig.8. The samples were heated from 30°C to 1100°C at a rate of 30 °C per minute. These graphs explain how catalyst weight continually varies as the temperature rises due to thermal treatment. The weight losses are attributed to the oxidation of the metals and the release of the adsorption moistures, volatile compound chemicals, and other substances, as seen from the DTG curve [24, 25]. The TGA curve (Fig.8(a)) of the nanocatalyst [NCM/AC] reveals that a losing weight of (3.4%) occurs between (94 - 160 °C) with the most significant weight loss rate reported at (100.3 °C), where the moisture in the sample had begun to volatilize. The lowest decomposition was seen in the samples reported in Fig.8 (b). At temperatures between 280 and 400 °C, decomposition reactions were seen (where the activated carbon started to decompose at 230.43 °C and reached its peak temperature at 350.21 °C) with a proportional losing weight of (4.7%), and the most significant increase of losing weight was seen at (305 °C). Later, losses were probably caused by hydroxyl convection and the breakdown of fiber, phosphoric acids, and hemicellulose [26, 27]. With a losing weight of (8.8%), a second breakdown process was noted between (400 and 780 °C) where the most significant rate happening at (580.7 °C). This thermal treatment temperature range's loss could also be attributed to the complete breakdown of hemicellulose, fiber, and oxidation [24]. The final stage of losing weight was (2.83%), which occurred between (800 and 900 °C), with the most significant rate seen at (833.5 °C). At a temperature of around 800°C, mass losses of the samples were also noticed, indicating that the lignin complex was decomposing, and this might be explained by the full cellulose breakdown and the conversion of metals. The (Thermo gravimetric analysis) TGA curve of the nanocatalyst [NCMM/AC] reveals that a losing weight of (3.2%) occurred between (73 - 180 °C) with the greatest losing weight rate reported at (99.5 °C). At temperatures between (300 and 380 °C), breakdown reactions were noticed with a proportional losing weight of (4.0%) where the most significant increase of losing weight was at (310.2 °C). The final breakdown process was losing weight (5.8%) between (540 and 890 °C), with the most significant rate occurring at (740.2 °C). This was explained by the full breakdown and the conversion of metals [25-27]. Generally, the stability of the magnetic adsorbents was also affected by the impregnation of magnetic particles. The weight losses of the NCMM/AC catalyst were lower than those obtained by NCM/AC catalyst, indicating that adding Mo increased the thermal stability of the catalyst generated. According to the findings, as the proportion of weight losses decreased, the impregnation of parent materials with NCMM magnetic particles strengthened the sample's thermal stability.

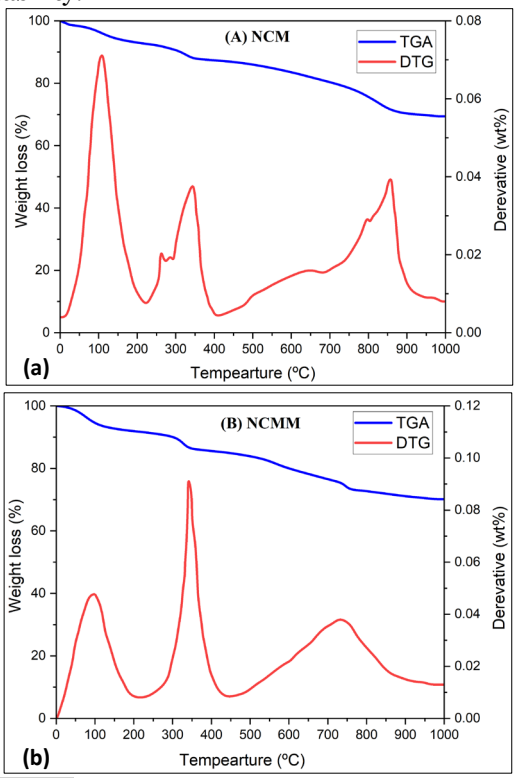

Fig. 8 TGA and DTG Curves of (a) NCM/AC and (b) NCMM/AC.

3.1.5. Fourier Transform Infrared Analysis (FTIR)

TIR spectroscopy was used to analyze the functional groups present in the synthesized activated carbons with the adsorption of metals (Ni (II), Co (II), Mn (II), and Mo) ions. The FTIR spectra of the AC, NCM/AC, and NCMM/AC samples are presented in Fig.9. A large band in the AC spectrum at 3443 cm^{-1} could be attributed to the stretching vibration of the hydroxyl group (O-H) due to the water molecules' vibration [28]. The aliphatic C-H stretch existence of the CH, CH_2, and CH_3 groups was responsible for the peak's prominence at 2932 cm^{-1}. The CH_2 symmetric stretching was attributed to the peak at 2853 cm^{-1}, and the presence of C=C groups caused the peak to appear at 2351 cm^{-1}. The two peaks were more pronounced in NCM/AC sample and even more in NCMM/AC sample than the AC sample. This indication proves that NCMM material was expected to show the highest activity among the other tested samples due to its highest functional groups [29]. The C=N stretching vibrations are associated with the peak at 2084 cm^{-1}. The peak visible at 1626 cm^{-1} can possibly be related to carboxylic acids' C=O stretching. C-H asymmetric and symmetric bending Figure vibrations are assigned to the band 1444cm^{-1} [30]. Peaks between 640 and 430 cm^{-1} were, however, attributed to metal oxide stretching vibration. The presence of the C-O group in the sample may cause a weak band in the 900–1300 cm^{-1} region. The stretching vibrations of the C-H out-of-plane band were connected to the band discovered at 836 cm^{-1}. All of the functions found in the AC were apparent in the FTIR spectra of NCM/AC and NCMM/AC, which suggests that metals were physically adsorbed onto the surface of the AC [31-33].

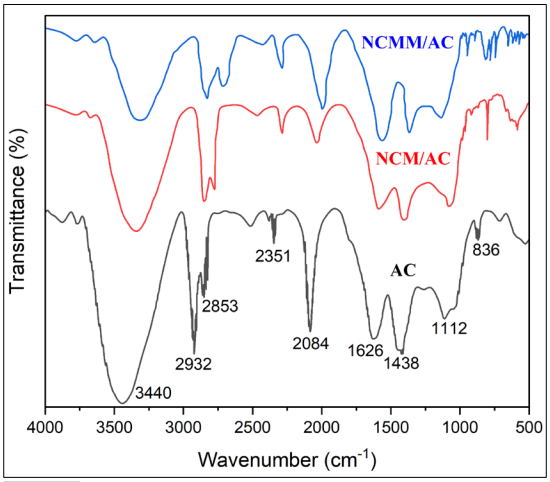

Fig. 9 FTIR of the Prepared AC, NCM/AC and NCMM/AC.

3.1.6.Analysis of X-ray Diffraction (XRD)

The most traditional technique that is widely used for portraying catalysts is X-ray diffraction (XRD). It can be employed to identify the crystalline state within catalysts. Fig. 10 demonstrates the transition metal doping impact on activated carbon (catalytic enhanced metals).

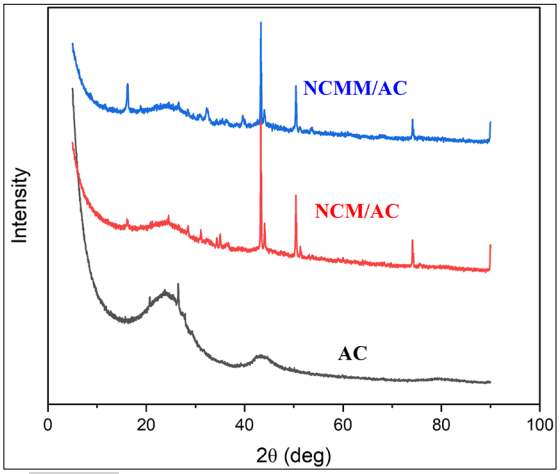

Fig. 10 XRD Analysis of the Prepared AC, NCM/AC and NCMM/AC.

The activated carbon creation is shown by the phase angles at the 2 theta coordinates of 25.67° and 43.28°. These peaks' forms may be seen in the created NCM and NCMM. NCMM and NCM caused the peak to appear between 51.00° and 75.34°. The most crucial noticeable evidence from this figure is the shifting of the 25.67 peak to the left of NCM material and even more of NCMM material, which may be attributed to the enhancement of the structural stability of the impregnated activated carbon with transition metals [30]. So, NCMM was expected to show superior activity among all.

3.2. Catalysts Evaluation Based on Batch Reactor

Concerning the oxidative desulfurization procedure on Iraqi whole cut oil (from initial boiling point to 345 °C), the activity of the prepared metals NCM and NCMM over AC was examined here. Under the following parameters, the air was an oxidant in a batch reactor at an airflow rate of 2 lit/min, reaction temperature = 90 °C, and reaction time = 60 min for both catalysts. It is well known that sulfur compounds are somewhat more polar than hydrocarbons with comparable structures. Sulphones and sulfoxide oxidize sulfur and have much more polarity than sulfur dioxide. More importantly, the conversion of sulphones from sulfides is typically much simpler and quicker than most hydrocarbons. Fig. 11 displays the experimental findings regarding catalyst activity in the oxidation process. It was evident from this figure that the catalysts prepared here can be used for sulfur removal from oil fractions depending on the results obtained. Also, the conversion of sulfur compounds increased with the catalyst stability via improving the catalyst's active sites by the molybdenum (Mo) materials under the same

conditions. The outcomes demonstrated that these catalysts exhibited the same behavior; however, the NCMM/AC catalyst exhibited higher activity than the NCM/AC catalyst under process conditions. Due to NCMM/AC's active compound loaded, which was the highest among catalysts, its activity was superior to that of the NCM/AC catalyst. This phenomenon is ascribed to the catalysts' activity linked to their high surface area.

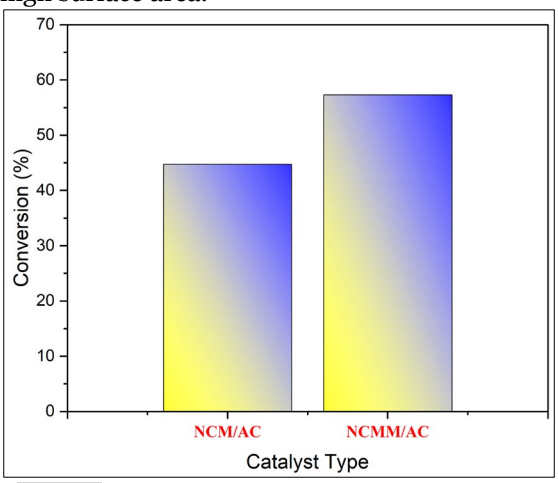

Fig. 11 Evaluation of the Catalysts NCM/AC and NCMM/AC via ODS Reaction.

As Mo was added, more active sites became available for the adsorption of refractory sulfur compounds. Additionally, the support that covered its surface filled the pores. The characteristics of the metal loaded, as well as the support material represented by AC, had a significant impact on the desulfurization process' effectiveness. The complex process of removing sulfur is governed mainly by the chemical interactions of the metals placed on the catalyst surface and the physical variables resulting from the adsorption behavior. Consequently, the acidic component or acidic site of AC support aided in removing the substituted sulfur compounds having alky hindrance. The Mo site increased the organ sulfur compounds removal possessing heteroatoms besides NCM.

4.CONCLUSIONS

The creation of a novel activated carbon (AC) produced from apricot shells (as) loaded with a mixture of metals Mn, Co, and Ni (NCM/AC); and Mn, Co, Ni, and Mo (NCMM/AC) using wetness impregnated method is described in this study (IWI). Regarding the environmental perspective, the generation of AC from AS is free of risk, economical, and eco-friendly. Based on the study's innovative technique for creating the (AC) from the least expensive basic ingredients (AS), it has been addressed those excellent results for nanomaterial with a high surface area of (1133.347 m^2/g) and excellent other characteristics can be achieved. Owing to the high pore volume and surface area and the great dispersion of the active metal, this procedure is useful for preparing the nanocatalysts, and the active chemical is primarily responsible for the catalyst's performance. The excellent metals loading onto the AC was established by textural characterization using FTIR, XRD, TGA, SEM-EDS, and S_{BET} and pore volume. The results also demonstrated that the nanocatalyst (NCMM/AC) removed more sulfur than the nanocatalyst (NCM/AC). The new homemade nanocatalysts (NCM/AC and NCMM/AC) could be used confidently in ODS reactions. They were clearly identified as the most significant catalyst when considering the aspects of process conversion received here. Improving the thermal stability and the activity of the NCM/AC can be enhanced by adding the molybdenum (Mo) material leading to an increase in the sulfur removal by the ODS reaction of the whole cut fuel.

REFERENCES

[1] Betiha M, Rabie A, Ahmed H, Abdelrahman A, El Shahat F. **Oxidative Desulfurization Using Graphene and its Composites for Fuel Containing Thiophene and its Derivatives: An Update Review**. *Egyptian Journal of Petroleum* 2018; **27**: 715–730.

[2] Prajapati R, Kohli K, Maity S. **Slurry Phase Hydrocracking of Heavy Oil and Residue to Produce Lighter Fuels: An Experimental Review.** *Fuel* 2021; **288:** 202– 228.

[3] Fahim M, Al-Sahhaf T, Elkilani A. **Fundamentals of Petroleum Refining**. 1st edition, Elsevier, New York, USA 2010.

[4] Chandra V. **An Evaluation of Desulfurization Technologies for Sulfur Removal from Liquid Fuels**. *RSC Advances* 2012; **2**: 759–783.

[5] Aysar TJ, Ban AAl-T, Mustafa AA, Shymaa AH, Iqbal MM. **Design of Novel Synthetic Iron Oxide Nano-Catalyst over Homemade Nano-Alumina for an Environmentally Friendly Fuel: Experiments and Modelling**. *Petroleum & Coal* 2022; **64**: 917–937.

[6] Shymaa AH, Amer TN,Qahtan AM, Layth TA, Aysar TJ, Iqbal MM. **Production of Green Fuel: A Digital Baffle Batch Reactor for Enhanced Oxidative Desulfurization of Light Gas Oil Using Nano-Catalyst in petroleum**. *Iranian Journal of Chemistry and Chemical Engineering* 2023; **42**: 740–753.

[7] Chen L, Li F. **Oxidative Desulfurization of Model Gasoline Over Modified Titanium Silicalite**. *Petroleum Science and Technology* 2015; **33**: 196–202.

[8] Li Z, Xu J, Li D, Li C. **Extraction Process of Sulfur Compounds from Fuels with Protic Ionic Liquids**. *RSC Advances* 2015; **21**: 15892–15897.

[9] Monai M, Montini T, Melchionna M. **The Effect of Sulfur Dioxide on The Activity of Hierarchical Pd-Based Catalysts in Methane Combustion**. *Applied Catalysis B: Environmental* 2017; **202**: 72–83.

[10] Ahmad S, Ahmad M, Naeem K, Humayun M, Sebt-E-Zaeem F. **Oxidative Desulfurization of Tire Pyrolysis Oil**. *Chemical Industry and Chemical Engineering Quarterly* 2016; **22**: 249–254.

[11] Bertleff B, Claußnitzer J, Korth W, Wasserscheid P, Jess A, Albert J. **Catalyst Activation and Influence of the Oil Matrix on Extractive Oxidative Desulfurization Using Aqueous Polyoxometalate Solutions and Molecular Oxygen**. *Energy & Fuels* 2018; **32**: 8683–8688.

[12] Yue D, Lei J, Zhou L, Du X, Guo Z, Li J. **Oxidative Desulfurization of Fuels at Room Temperature Using Ordered Meso/Macroporous $H_3PW_{12}O_{40}/SiO_2$ Catalyst with High Specific Surface Areas**. *Arabian Journal of Chemistry* 2020; **13**: 2649–2658.

[13] Bertleff B, Claußnitzer J, Korth W, Wasserscheid P, Jess A, Albert J. **Extraction Coupled Oxidative Desulfurization of Fuels to Sulfate and Water-Soluble Sulfur Compounds Using Polyoxometalate Catalysts and Molecular Oxygen.** *ACS Sustainable Chemistry & Engineering* 2017; **5**: 4110–4118.

[14] Ji H, Ju H, Lan R. **Phosphomolybdic Acid Immobilized on Ionic Liquid-Modified Hexagonal Boron Nitride for Oxidative Desulfurization of Fuel**. *RSC Advances* 2017; **7**: 54266–54276.

[15] Mohammed HJ, Aysar TJ, Al-Tabbakh BA, Hussein HM. **Preparation of Synthetic Composite Nano-Catalyst for Oxidative Desulfurization of Kerosene**. *Energy Sources, Part A: Recovery, Utilization, and Environmental Effects* 2023; **45**: 1672–1685.

[16] Jarullah AT, Ahmed AM, Hussein HM, Ahmed AN, Mohammed HJ. **Evaluation of Synthesized Pt/HY-H- Mordenite Composite Catalyst for Isomerization of Light Naphtha**. *Tikrit Journal of Engineering Sciences* 2023; **30**(1): 94–103.

[17] Jarullah AT, Ahmed AA, Ban AA, Ahmed AM. **Design of New Composites Nano-Catalysts for Naphtha Reforming Process: Experiments and Process Modeling**. *Tikrit Journal of Engineering Sciences* 2023; **30**(2): 46–59.

[18] Ahmed GS, Jarullah AT, Al-tabbakh BA, Mujtaba IM. **Design of an Environmentally Friendly Reactor for Naphtha Oxidative Desulfurization by Air Employing a New Synthetic Nano-Catalyst Based on Experiments and Modeling**. *Journal of Cleaner Production* 2020; **257**: 120436, (1-38).

[19] Jasim IH, Amer TN, Jarullah AT, Mustafa AA, Shymaa AH, Mujtaba IM. **Design Of New Nano-Catalysts and Digital Basket Reactor for Oxidative Desulfurization of Fuel: Experiments and Modelling**. *Chemical Engineering Research and Design* 2023; **190**: 634–650.

[20] Ertl G, Knozinger H, Weitkamp J. **Handbook of Heterogeneous Catalysis**. Wiley-VCH Verlag GmbH & Co, Germany 1997.

[21] Jarullah AT, Aldulaimi SK, Al-Tabbakh BA, Mujtaba IM. **A New Synthetic Composite Nano-Catalyst Achieving an Environmentally Friendly Fuel by Batch Oxidative Desulfurization.** *Chemical Engineering Research and Design* 2020; **160**: 405-416.

[22] Petrova B, Budinova T, Tsyntsarski B, Kochkodan V, Shkavro Z, Petrov N. **Removal of Aromatic Hydrocarbons from Water by Activated Carbon from Apricot Stones**. *Chemical Engineering Journal* 2010; **165**: 258-264.

[23] de Mello S, Sobrinho EV, da Silva T, Pergher SBC. **V or Mn Zeolite Catalysts for the Oxidative Desulfurization of Diesel Fractions Using Dibenzothiophene as a Probe Molecule: Preliminary Study**. *Molecular Catalysis* 2020; **482**: 100495.

[24] Girgis B, El-Hendawy A. **Porosity Development in Activated Carbons Obtained from Date Pits Under Chemical Activation with Phosphoric Acid**. *Microporous and Mesoporous Materials* 2002; **52**: 105–117.

[25] Pourkhalil M, Moghaddam A, Rashidi A, Towfighi J, Mortazavi Y. **Preparation of Highly Active Manganese Oxides Supported on Functionalized MWNTs for Low Temperature NO_x Reduction with NH_3**. *Applied Surface Science* 2013; **279**: 250–259.

[26] Haw K, Abu Bakar W, Ali R, Chong J, Kadir A. **Catalytic Oxidative Desulfurization of Diesel Utilizing Hydrogen Peroxide and Functionalized-Activated Carbon in A Biphasic Diesel– Acetonitrile System**. *Fuel Processing Technology* 2010; **91**: 1105–1112.

[27] Zhao C, Jiang E, Chen A. **Volatile Production from Pyrolysis of Cellulose, Hemicellulose and Lignin**. *Journal of the Energy Institute* 2017; **90**: 902–913.

[28] Contescu I, Adhikari P, Gallego C, Evans D, Biss E. **Activated Carbons Derived from High-Temperature Pyrolysis of Lignocellulosic Biomass**. *C: Journal of Carbon Research* 2018; **4**(3): 51, (1-16).

[29] Saleh A. **Isotherm, Kinetic, and Thermodynamic Studies on Hg (II) Adsorption From aqueous Solution by Silica-Multiwall Carbon Nanotubes**. *Environmental Science and Pollution Research* 2015; **22**: 16721–1673.

[30] Tchalala R, El-Demellawi K, Abou-Hamad E. **Hybrid Electrolytes Based on Ionic Liquids and Amorphous Porous Silicon Nanoparticles: Organization and Electrochemical Properties**. *Applied Materialstoday* 2017; **9**: 10–20.

[31] Saleh A. **The Influence of Treatment Temperature on the Acidity of MWCNT Oxidized by HNO_3 or a Mixture of HNO_3/H_2SO_4**. *Applied Surface Science* 2011; **257**: 7746–7751.

[32] Bazrafshan A, Hajati S, Ghaedi M. **Synthesis of Regenerable $Zn(OH)_2$ Nanoparticleloaded Activated Carbon for the Ultrasound-Assisted Removal of Malachite Green: Optimization, Isotherm and Kinetics**. *RSC Advances* 2015; **5**: 79119–79128.

[33] Abdul-Kadhim W, Deraman M, Abdullah S, Tajuddin S, Yusoff M, Taufiq-Yap Y, Rahim M. **Efficient and Reusable Iron-Zinc Oxide Catalyst for Oxidative Desulfurization of Model Fuel**. *Journal of Environmental Chemical Engineering* 2017; **5**: 1645–1656.